An in-process ultrasonic approach to investigating the relaxation of orientation and disorientation of polymer melts

Li, Jiang; Sun, Zhigang; Tatibouet, Jacques; Jen, Cheng-Kuei

Publisher's version / Version de l'éditeur:
https://doi.org/10.1002/pen.21023
Polymer Engineering and Science, 48, 5, pp. 987-994, 2008-05

An In-Process Ultrasonic Approach to Investigating the Relaxation of Orientation and Disorientation of Polymer Melts

Jiang Li,[1,2] Zhigang Sun,[1] Jacques Tatibouët,[1] Cheng-Kuei Jen[1]
[1] *Industrial Materials Institute, National Research Council Canada, Boucherville, Quebec J4B 6Y4, Canada*

[2] *Department of Electrical and Computer Engineering, McGill University, Montreal, Quebec H3A 2A7, Canada*

The orientation and relaxation behaviors of a low-density polyethylene melt and polypropylene melts with different melt indices undergoing a shear flow in a restricted channel were investigated by using ultrasound. A capillary rheometer was used to force the polymer melt through a slit die equipped with pressure, temperature, and ultrasound sensors, and the variation of ultrasound velocity traversing the melt was measured. Experimental results revealed that due to different mechanisms involved, the relaxations of orientation and disorientation processes show different dependences of ultrasound velocity on shear rate, temperature, and melt index. POLYM. ENG. SCI., 48:987–994, 2008. Published 2008 Society of Plastics Engineers

INTRODUCTION

It is well known that many properties, such as mechanical and optical properties, of polymer materials are strongly influenced by shear induced molecular orientation occurring under various polymer melt processing conditions. During such macroscopic deformation, the orientation of isotropic network of polymer chain segments becomes anisotropic with ability to adopt different conformations, from a coil to an extended chain. The disorientation is an opposite process to orientation by which the molecular chains recoil gradually after the cessation of shear. Apparently, the developments of molecular orientation and disorientation depend on the relaxation process due to the undergone great friction when macromolecular chains move. The relaxation phenomena in polymers have been the subject of research for many years, due to their importance in the modeling of polymer processing and analysis of processing experiments [1–3].

Traditionally, polymer relaxation is characterized by a spectrum of multiple relaxation times corresponding to various modes of relaxation a polymer chain can undergo. The longest relaxation time corresponds to the relaxation of a whole chain, while the shorter ones correspond to the relaxation of short parts of the macromolecules. In this paper, we are particularly interested in the relaxation behavior at molecular chain level. Dynamic rheometers are the most used means for providing relaxation time spectrum of polymer melts [4–6]. However, since they only generate small scale melt deformation during measurements, the relaxation time at macromolecular level calculated from the terminal region (i.e., at low frequencies) of linear viscoelastic properties is not directly representative of the relaxation of the orientation or disorientation of molecular chains undergoing large deformation. As discussed in [7], the basic understanding of the mechanisms involved in orientation (disorientation) and its subsequent relaxation is based on the reptation theory by de Gennes and on the chain relaxation model developed by Doi and Edward. Some computer simulations were performed to predict the relaxation behavior of polymer melts according to the concept of reptation [8, 9]. Recently, experimental characterization of molecular relaxation behavior is of particular interest for both industrial applications and fundamental understanding of the molecular mechanisms involved in polymer deformation. Several experimental techniques such as X-ray diffraction [10, 11], NMR spectroscopy [12, 13], and polarized infrared dichroism [11, 14, 15] have been applied extensively to measure the orientation (disorientation) and relaxation in polymers on a molecular scale in order to correlate the microstructure to the macro physical properties. The studied objects were solid polymer samples, which were obtained by immediate quenching in the glassy state after being allowed to relax in the melt state for different time intervals in order to freeze the corresponding molecular orientation. These are off-line methods and cannot provide a continuous observation on the sample during melt

Correspondence to: Zhigang Sun; e-mail: zhigang.sun@imi.cnrc-nrc.gc.ca
DOI 10.1002/pen.21023
Published online in Wiley InterScience (www.interscience.wiley.com).

deformation. The degree of orientation of injection-molded parts at the solidification stage has been studied by using ultrasonic shear wave transducers [16, 17]. Again, the method only applies to solid samples. Among in-line methods, fluorescence anisotropy measurements have been developed for studying molecular orientation of polymer melt under a shear force. The technology uses polarized light sources to look at the fluorescence anisotropy of fluorescent dye molecules entangled with the polymer molecules and uses the variation in the anisotropy of the die molecules as an indication of change in the molecular orientation of the polymer melt under the shear force [18, 19]. Since the dye molecules may be too small to be well engaged in the entanglement network of the host polymer matrix, this technology may not be sensitive enough to probe macromolecular scale molecular orientation. Dielectric sensing is another powerful approach to in-line polymer process monitoring. Dielectric relaxation spectroscopy has been used to monitor dipolar relaxation behavior of the polymer matrix in nylon/clay nanocomposites during extrusion [20]. The technique was able to measure molecular chain segment relaxation but did not measure relaxation of the entire molecules.

In this article, we report a novel ultrasonic method for real-time study of the relaxations of orientation and disorientation of polymer melts. Ultrasonic technology offers the advantages of being noninvasive, nonintrusive, quick in response, and highly sensitive to micro-structural changes. These advantages make ultrasonic technology suitable for many real-time process diagnosis needs [21–24].

The velocity of longitudinal ultrasonic waves in a polymer melt can be expressed as a function of the bulk modulus, K, and the density, ρ, of the melt:

$$C = \sqrt{K/\rho} \tag{1}$$

When undergoing shearing stress, the macromolecular chains tend to align parallel to the direction of shear flow. The modulus in the direction perpendicular to shear flow decreases compared with an unoriented polymer melt, resulting in a decrease in the velocity of ultrasound in the melt propagating perpendicularly to the shear flow direction. Similarly, the disorientation after the cessation of shear will result in an increase in the velocity of ultrasound propagated perpendicularly to the shear flow. This forms a theoretical basis for correlating the change of ultrasonic velocity to the relaxation of orientation or disorientation. The objective of this work is to establish a basic understanding of processing-orientation (disorientation)-relaxation-ultrasonic velocity relationships.

EXPERIMENTS

The experimental setup is shown in Fig. 1. A slit die was fit to the barrel exit of a Rosand capillary rheometer. The slit die had a rectangular opening of 13.35 mm by 2.0 mm, a length of 140 mm, and was equipped with two ultrasound sensors (denoted by "US" in the figure) located in cross-section I, one melt pressure sensor (denoted by "PS2") and a melt temperature sensor (denoted by "Tmelt") in cross-section II, and another pressure sensor (denoted by "PS3") and a die temperature sensor (denoted by "Tdie") in cross-section III. The cross-sections I, II, and III were equidistantly located from the exit of the slit die. The slit die temperature was controlled with a wrapped-on heating jacket. Except the die temperature sensor, all other sensors were flush-mounted in three cross-sections and perpendicularly to the wider surfaces of the slit. The ultrasound sensors were axially aligned, but on the opposite sides of the slit. The temperature sensors were J-type thermocouples, and the pressure sensors were Dynisco melt pressure transducers. For ultrasonic measurements, one of the ultrasound sensors transmitted 5-MHz ultrasonic waves to the molten polymer. The transmitted ultrasonic waves were then received by the ultrasound sensor on the other side of the slit. The pressure, temperature, and ultrasound signals were acquired simultaneously at every 0.1 sec with a PC-based ultrasound system custom-designed and built in the laboratory. By measuring the traveling time of ultrasound through the polymer, the ultrasound velocity in the molten polymer was obtained. The melt pressure in the cross-sec-

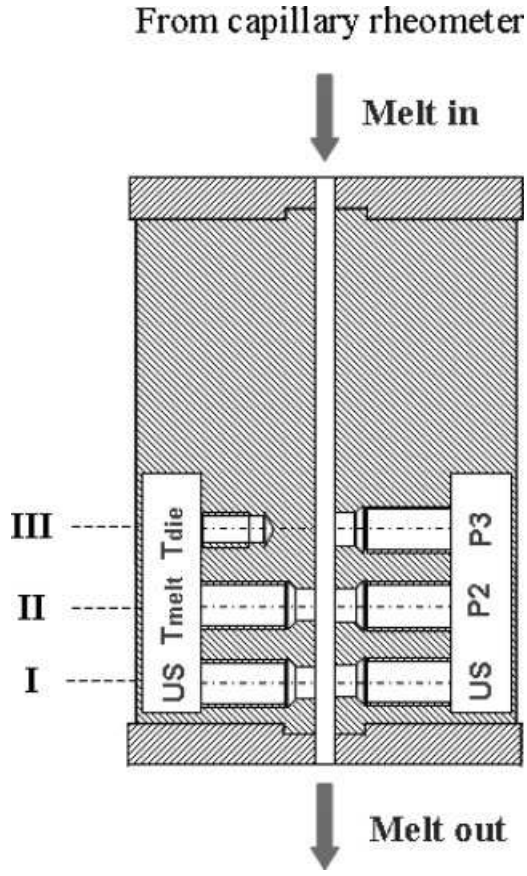

FIG. 1. Instrumented slit die.

 DOI 10.1002/pen

TABLE 1. Polymer resins used in this work and some of their characteristics.

Sample	Melt flow index (MFI)	Density (g/cm^3)	Polymerization type	Grade	Producer
LDPE	3.2	0.922		LF-0323-A	Novachemicals
PP-1	1.4	0.902	Copolymerization	SV152	Basell
PP-2	12	0.902	Homopolymerization	PDC1274	Basell
PP-3	12	0.902	Copolymerization	SB821	Basell
PP-4	100	0.902	Copolymerization	SC973	Basell

tion I probed by the ultrasound sensors was obtained by extrapolating the pressure readings provided by the pressure sensors located in the cross-sections II and III.

The materials include a low density polyethylene (LDPE) and four polypropylenes (PP) with physical properties listed in Table 1. The experiments were carried out at five set temperatures, namely, 166, 167, 200, 210, and 220°C. For each test, the set temperatures for the rheometer barrel and the slit die were maintained at the same value. The polymer melt was forced through the slit die by means of a piston moving in the rheometer barrel. Nine piston speeds in the range of 10 to 90 mm/min were selected in this study.

The linear viscoelastic properties of LDPE samples were measured on a Rheometric Scientific® rheometer with a 25-mm diameter parallel plate geometry. The samples were examined at five different temperatures, namely, 166, 167, 200, 210, and 220°C, and at 15 oscillating frequencies between 0.1 and 100 rad/sec.

RESULTS AND DISCUSSION

Changes in Temperature, Pressure, and Ultrasound Velocity With Time

As can be seen from *Eq. 1*, the ultrasound velocity in a polymer melt is determined by the bulk modulus and mass density of the melt. When subjected to a shear flow, the molecular chains of a polymer melt can be forced to orient along the shear flow direction. After the cessation of flow, the macromolecules will undergo a disorientation process by which the molecular chains recoil with time. These changes in microstructure will affect the bulk modulus, and to a much lesser extent, the melt density, leading to a change in the velocity of ultrasound propagating in the polymer melt. However, variations in the temperature and pressure also affect sound velocity through their effects on bulk modulus and density. It has been observed that within the temperature and pressure variation ranges encountered during the tests, the effects of temperature and pressure on ultrasound velocity can be reasonably well factored into the following equation via a linear dependence of ultrasound velocity on temperature and pressure:

$$C(S,T,P) = C(S_0,T_0,P_0) + C_T(T-T_0) + C_P(P-P_0) + f(S_0,S) \quad (2)$$

where $C(S_0,T_0,P_0)$ is the ultrasound speed measured at temperature T_0 and pressure P_0 when the melt is in a static state denoted by S_0, $C(S,T,P)$ is the sound speed measured at temperature T and pressure P when the melt is in a state S, C_T, and C_P are the sensitivity coefficients of ultrasound velocity to temperature and pressure changes, and $f(S_0,S)$ is the variation of ultrasound velocity caused by the material structure change from state S_0 to state S that is not accounted for by the linear temperature and pressure dependences in *Eq. 2*. We use C_R to replace $f(S_0,S)$ in *Eq. 2* with the subscript "R" denoting the velocity variation relative to the initial state and with pressure and temperature effects cancelled out, and we have

$$C_R = C(S,T,P) - C(S_0,T_0,P_0) - C_T(T-T_0) - C_P(P-P_0) \quad (3)$$

The coefficients C_T and C_P were obtained through a separate study in which the ultrasound speed in the polymer melt were measured under various temperatures and pressures and when the melt was in a static state [25].

As an example, Fig. 2 shows typical behaviors of melt temperature, pressure, ultrasound velocity C during a test carried out at set temperatures of 167°C and a shear rate of 23.1 sec^{-1}. The process is divided into three stages,

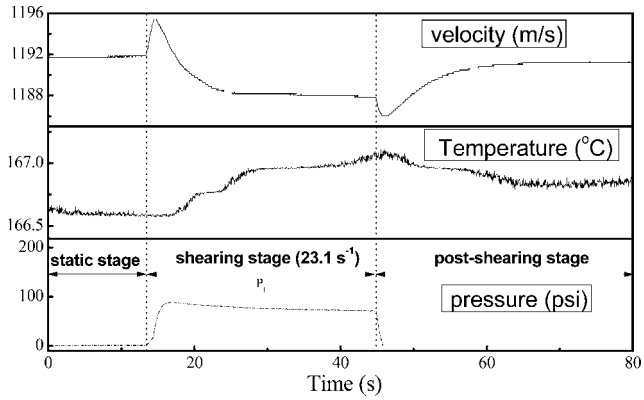

FIG. 2. Evolution of ultrasound velocity, melt temperature, and melt pressure during a test carried out at set temperatures of 167°C and a shear rate of 23.1 sec^{-1}.

namely, static stage (from 0 to 13.5 sec), shearing stage (from 13.5 to 44.9 sec) during which the piston was pushing the melt through the slit die, and post-shearing stage (from 44.9 sec to the end) during which the movement of the piston was stopped. One can see that the melt temperature increases slightly (about 0.5°C) during the shearing stage due mainly to shear heating, then decreases gradually in the post-shearing stage. According to one of our separate studies, this temperature rise can lead to a small decrease of about 1 m/sec in ultrasound speed. At the beginnings of shearing and post-shearing stages, the pressure changes sharply. Under the effect of pressure, the ultrasound velocity also changes sharply in the direction of pressure change. However, after the pressure stabilizes, the ultrasound velocity evolves in an opposition direction, due to the variation in the degree of molecular chain orientation. It should be pointed out that the ultrasound velocity carries almost the same value at the end of the post-shearing stage as that in the static stage, suggesting that the original molecular structure was completely recovered at the end of the process. The above analysis demonstrates clearly that the ultrasound velocity can reveal the structural information related to the relaxations of molecular orientation and disorientation.

Molecular Orientation of LDPE and its Relaxation

The effects of pressure and temperature on the ultrasound velocity displayed in Fig. 2 can be cancelled out by using *Eq. 3*. The resulting C_R for the shearing stage is shown in Fig. 3. For easier presentation, the starting point of the shearing stage is taken as the origin of the time axis of the figure. The experimental data shown in Fig. 3 can be reasonably well described by the following relaxation model:

$$C_R(t) = C_\infty(1 - e^{-t/\tau}) \tag{4}$$

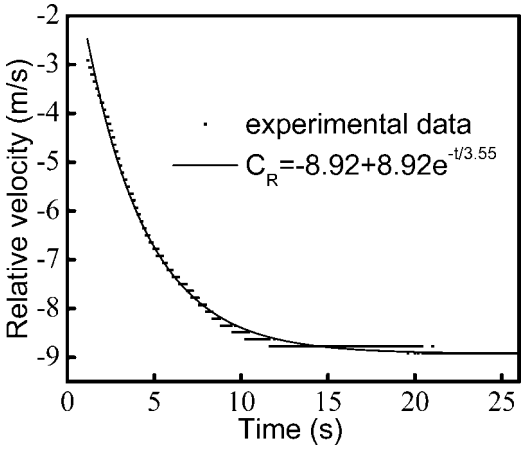

FIG. 3. Modeling of the relation between relative velocity (C_R) and process time during orientation at a shear rate of 23.1 sec^{-1} and a temperature of 167°C.

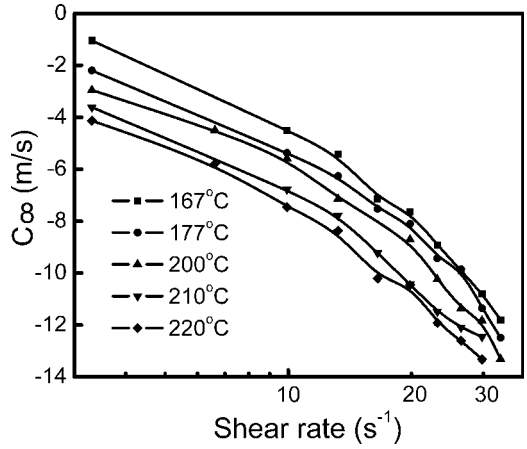

FIG. 4. Shear rate and temperature dependences of C_∞ during orientation.

where τ is the relaxation time and C_∞ represents the chain orientation induced change of ultrasound velocity after the melt flow reaches a steady state. By using least squares fitting, we obtained $C_\infty = 8.92\ m/s$, and $\tau = 3.55s$.

Figure 4 provides a comparison among the values of C_∞ measured under different shear rates and different temperatures. In this article, the shear rate refers to the apparent shear rate at the wall calculated by $\dot{\gamma}_A = 6Q/h^2w$ with Q being the volume flow rate, and h and w being the slit height and width, respectively. The flow rate was determined from the displacement speed and the diameter of the piston of the capillary rheometer. In the figure, as in the remaining figures of the article, the discrete points represent the measured data whereas the lines represent the curves fitted to the data points. The fitted curves either serve as a visual aid to indicate the tendency of variation of a particular parameter, or represent a mathematical model of the experimental data. The absolute value of C_∞ increases with increasing shear rate. Every increase in melt temperature results in a downward shift of the curve (i.e. an increase of the absolute value of C_∞). Molecular orientation is not a spontaneous process. The positive effects of shear rate and temperature on the degree of orientation can be well explained by the facts that kinetically, a stronger shearing force results in a larger deformation of macromolecules, and thermodynamically, an increase in temperature reduces the potential energy of molecular motion.

It should be pointed out that the shear rates investigated in this work were limited to very low values. The limiting factor was the use of a thermocouple for melt temperature measurement. It is well-known that the reading of a thermocouple could be much affected by the temperature of the die (or barrel) on which it is mounted and may not be representative of the true melt temperature [26]. One way to reduce the discrepancy between the read temperature and the true melt temperature was to make the melt temperature as close to the die temperature as

 DOI 10.1002/pen

possible by limiting the shear rate in such a way that the melt temperature rise caused by shear heating becomes negligible. According to the research published in [27], the temperature reading error caused by shear heating effect may be negligible in the present work. A fluorescence temperature measurement technique as that developed by the authors of [27] could allow us to go much higher in shear rate in the future work.

Molecular orientation can also affect melt viscosity. Figure 5 displays corresponding melt viscosities measured at the same time of ultrasonic tests. In this article, the melt viscosity refers to the apparent shear viscosity calculated from $\eta_A = \Delta P h^3 w/12LQ$, where ΔP and L are respectively the pressure drop and the center-to-center distance between pressure sensors PS3 and PS2 (see Fig. 1), h, w, and Q are respectively the slit height, slit width, and the volume flow rate and were defined earlier. The influence of shear rate and temperature on viscosity is totally reverse to that on C_∞. The viscosity decreases with increasing temperature and shear rate. Since at high melt temperatures as is the case of this study, a decrease in melt viscosity indicates a decrease in melt modulus, whereas an increase in the absolute value of C_∞ (or decrease of ultrasound speed) with increasing temperature and shear rate is also a consequence of reduced modulus, both ultrasonic and viscosity measurements point to the same direction. However, different from ultrasonic measurement which is capable for following instantly variation of polymer structure, viscosity measurement is usually conducted under steady state and as a consequence it is not a practical tool for studying the transient behavior involved in a relaxation process.

Figure 6 reveals the effects of shear rate and temperature on orientation relaxation time. The relaxation time decreases moderately with increasing shear rate at different temperatures. The dependence of relaxation time on temperature is not obvious compared to that on shear rate. Overall, the relaxation process is faster at higher temperatures in the range from 167 to 220°C. However, the influence of temperature on relaxation time is more pronounced at the lower end of shear rate. At high shear rates, all the relaxation times fall in the range between 2 and 3 sec. The data seem to suggest a convergence of the relaxation curves to a limiting point at higher shear rates, independently of temperature. Obviously, this cannot be explained by the classical WLF equation [28, 29] that predicts strong temperature dependence of relaxation time near glass transition temperature.

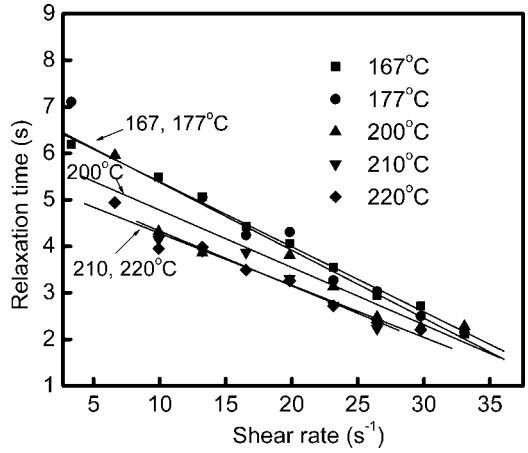

FIG. 6. The shear rate and temperature dependences of relaxation time of orientation.

Molecular Disorientation of LDPE and its Relaxation

Molecular disorientation takes place in the post-shearing stage, after the cessation of shear flow. The molecular disorientation causes a slow increase in ultrasonic velocity as shown in Fig. 2. The relaxation process of disorientation was investigated through the same approach described earlier for the orientation process except that the following relaxation model is used to describe the experimental data:

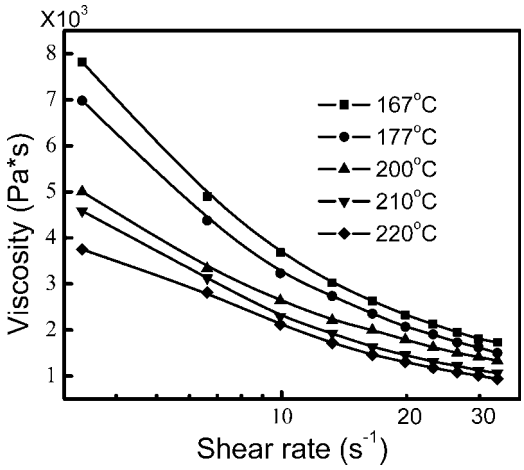

FIG. 5. Apparent viscosity versus shear rate at different temperatures measured during the orientation stage.

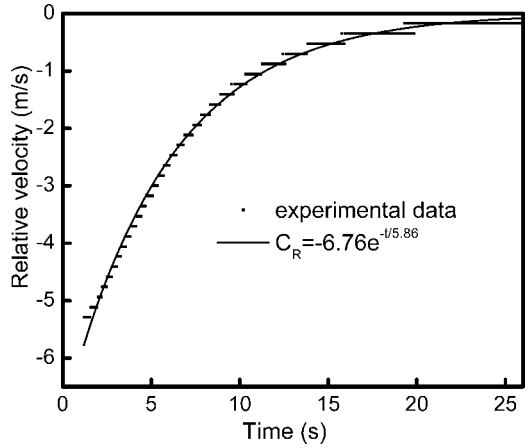

FIG. 7. Modeling of the relation between relative velocity (C_R) and process time during disorientation at a shear rate of 23.1 sec^{-1} and a temperature of 167°C.

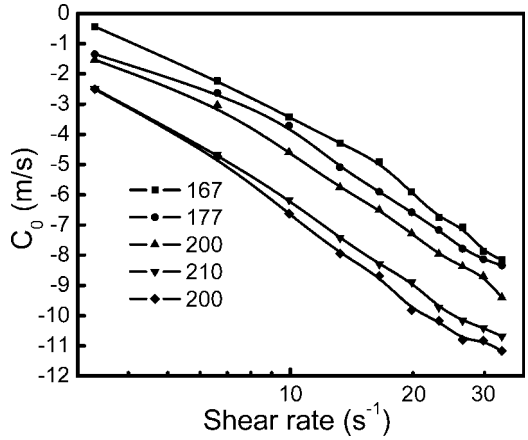

FIG. 8. The shear rate and temperature dependence of C_0 during disorientation.

$$C_R(t) = C_0 e^{-t/\tau} \tag{5}$$

where the starting point of the post-shearing stage was taken as the origin of time counter, and C_0 represents the chain orientation induced change of ultrasound velocity with respect to that after disorientation is completely relaxed. The evolution of C_R corresponding to the post-shearing stage displayed in Fig. 2 is shown in Fig. 7 in which the values of C_0 and τ are 6.76 m/sec and 5.86 sec, respectively. Note that the relaxation time of disorientation is greatly different from that of orientation. This is attributed to the fact that thermodynamically the molecular disorientation is a spontaneous process with distinct relaxation mechanisms from that of orientation. The measured relaxation times seemed quite long compared to some published data (for example those in Ref. 20). This could be attributed to the fact that we were measuring the relaxation time of entire molecular chains instead of that of chain segments.

Figures 8 and 9 show the influence of shear rate and temperature on C_0 and the relaxation time of disorientation, respectively. For the disorientation process, the evolutions

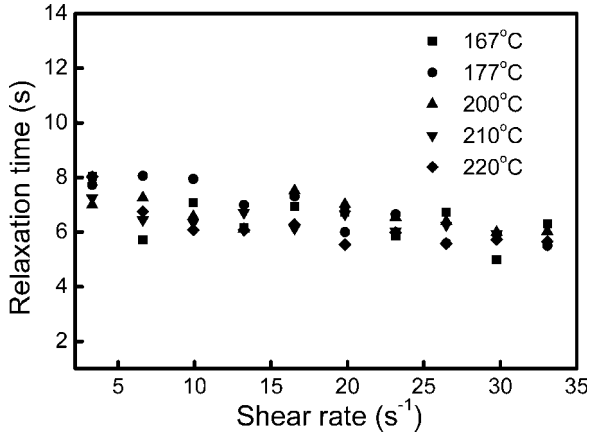

FIG. 9. Shear rate and temperature dependences of relaxation time during disorientation.

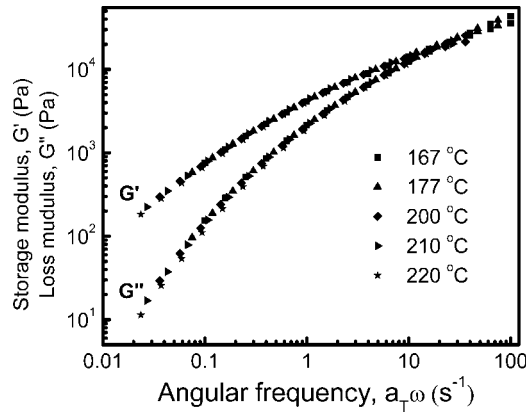

FIG. 10. Dynamic moduli of an LDPE as functions of angular frequency. Reference temperature is 167°C.

of C_0 versus shear rate and temperature behave very similarly to those of C_∞ in the orientation process. However, the temperature and shear rate dependence of the relaxation time appears negligible in the disorientation process compared to the orientation process. This coincides with the finding by Wiberg et al. that the relaxation of thermotropic liquid crystalline copolyester was independent of temperatures above 275°C [11]. This suggests that the relaxation time of the disorientation process of a polymer melt could be advantageously used as an intrinsic property of the polymer owing to its insensitiveness to shear rate and temperature. This needs to be confirmed by further studies.

The relaxation behavior of the LDPE was also investigated through rheological measurements carried out on the Rheometric Scientific rheometer. Figure 10 displays the variations of storage modulus G' and loss modulus G'' of the LDPE at a reference temperature of 167°C as functions of $a_T\omega$, with a_T being the shift factor used to obtain a master curve, and ω the angular frequency. From these data, the zero shear viscosity η_0 and steady state compliance J_e^0 can be obtained, and the weight average viscoelastic relaxation time, τ_w, can be determined as [30]

$$\tau_w = \eta_0 J_e^0 \tag{6}$$

According to [30], τ_w can be used for estimating the average time of stress decay subsequent to a sudden shear deformation of a melt. Since this stress decay is also the consequence of spontaneous movement of molecular chains, the value of τ_w should be comparable with the

TABLE 2. Values of some terminal viscoelastic parameters of LDPE at 167°C and the corresponding average relaxation time obtained by real-time ultrasonic measurement.

Zero shear viscosity η_0 (pa s)	Steady state compliance J_e^0 (pa^{-1})	Weight average viscoelastic relaxation time τ_w (sec)	Average relaxation time determined with ultrasound τ (sec)
8.8×10^3	4.9×10^{-4}	4.3	6.3

DOI 10.1002/pen

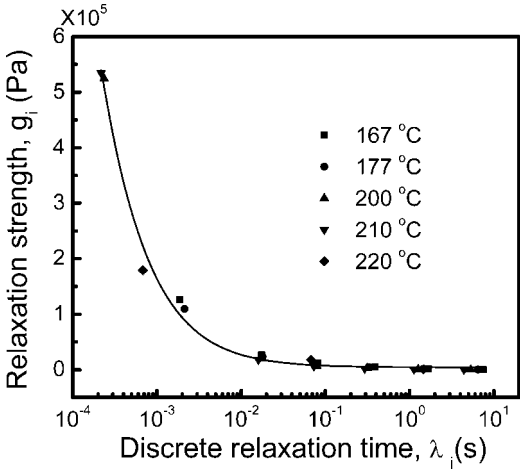

FIG. 11. Discrete relaxation spectra of LDPE at different temperature.

relaxation time observed in the disorientation process. The values of η_0, J_e^0, and τ_w calculated at 167°C are listed in Table 2. Also listed in the table is the average of the relaxation times at 167°C displayed in Fig. 9. As can be seen in the table, the value of τ_w, 4.3 sec, estimated from the terminal region of linear viscoelastic properties (which are manifested through small scale deformations) is quite close to the large scale macromolecular level relaxation time of disorientation, 6.3 sec, determined by real-time ultrasonic measurement.

From the storage and loss moduli, the relaxation time spectra were calculated using a nonlinear regression method [4]. Figure 11 shows the results. The spectra of discrete relaxation time at different temperatures appear to fall on the same curve. This is a strong indication that the influence of temperature on the relaxation time of the LDPE melt is negligible in the investigated temperature range. Similar observations have been reported in [31]. This is in agreement with our observations that the relaxation times of the disorientation processes investigated in this work were insensitive to temperature variation.

Orientation and Disorientation of PPs and Their Relaxations

Figure 12 shows how the degrees and relaxation times of the orientation and disorientation processes of four PPs listed in Table 1 vary with shear rate and melt flow index (MFI). All the tests were carried out at 200°C. Similar to the LDPE case, the relaxation time of orientation decreases with shear

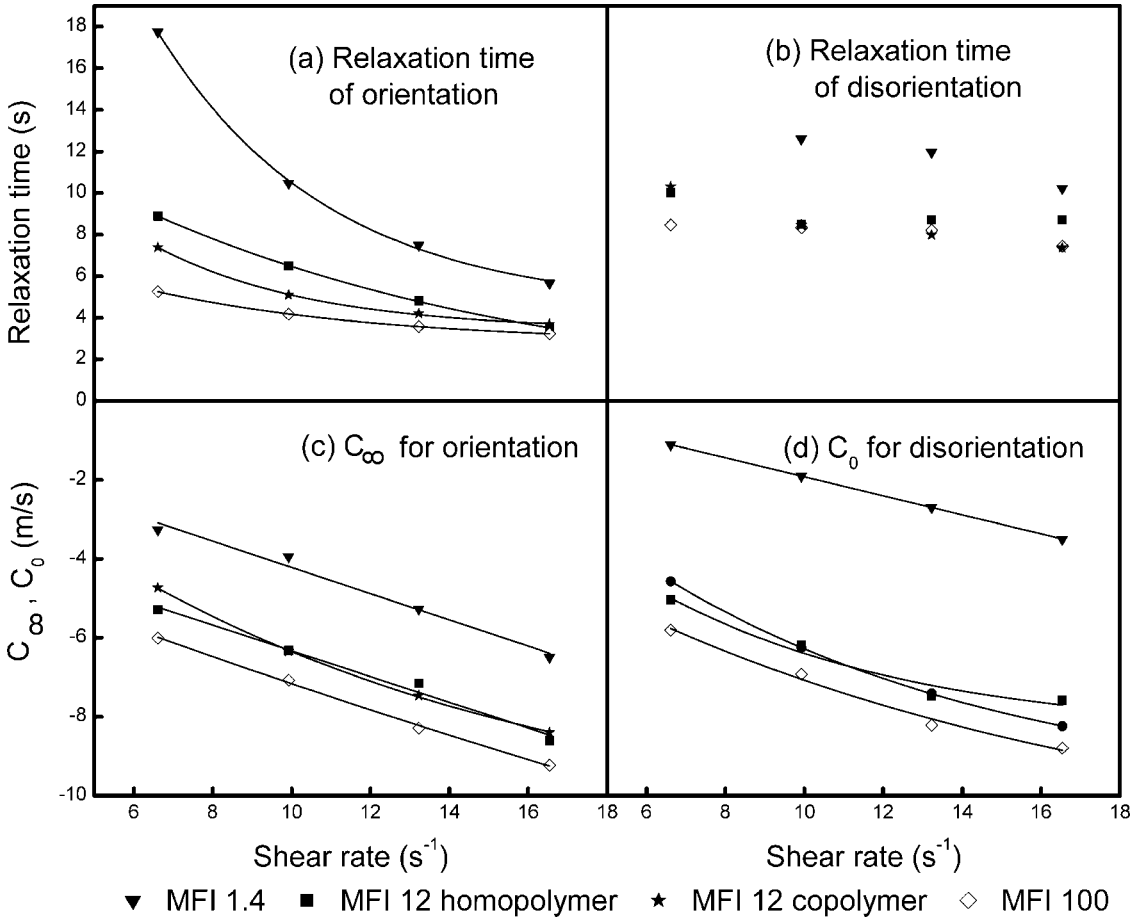

FIG. 12. Variations with shear rate and melt flow index of the degree and relaxation time of the orientation and disorientation processes of four PPs listed in Table 1 at 200°C.

rate when the shear rate is small. When the shear rate becomes larger, the relaxation time soon reaches a constant level (Fig. 12a). The higher the viscosity is (as manifested by a smaller MFI), the longer is this relaxation time and the more pronounced is the dependence of this relaxation time on shear rate. Comparing MFI 12 copolymer with MFI 12 homopolymer, shorter relaxation time was found with the former. This could be attributed to a faster molecular movement induced by the PE phase in the copolymer. For the disorientation processes, there is no clear dependence of relaxation time on shear rate, as is in the case of LDPE disorientation processes (Fig. 12b). The difference in the behaviors of orientation and disorientation relaxation times versus shear rate indicates that the mechanisms involved in the two processes are different. As also can be seen in Fig. 12(b), the relaxation time of disorientation process is not sensitive to MFI, and only shows noticeable difference when the difference of MFI is quite large. The evolutions versus shear rate of the degrees of molecular orientation and disorientation, as measured by the absolute values of C_∞ and C_0 respectively, are shown in Fig. 12c and d. The degrees of orientation and disorientation increase with shear rate. At higher MFI, larger degrees of molecular orientation and disorientation were observed. This is in accordance with the observations made in Figs. 4 and 8 that the degrees of orientation and disorientation increased with temperature, given that a rise in temperature results in a decrease in viscosity.

CONCLUSIONS

Macromolecular chain orientation and disorientation processes induced by first imposing a shear flow to a polymer melt and then stopping the flow have been investigated with ultrasound. The ultrasonic measurement is based on the principle that a change in molecular chain orientation can result in a change in the bulk modulus of the melt, which in turn leads to a change in the velocity of ultrasound propagating in the melt. By measuring the variation of ultrasound velocity, the degree and relaxation time of macromolecular chain orientation and disorientation of one LDPE and four PP samples were determined. It has been found that (1) the degrees of macromolecular orientation and disorientation increase with an increase either in shear rate, or in temperature, or in melt flow index; (2) The relaxation time of an orientation process, which originates from the exerting of an external force to the melt, decreases with increasing shear rate and temperature; the dependence of this relaxation time on temperature is more pronounced at lower shear rate; (3) The relaxation time of a disorientation process, which is spontaneous in nature, appears to be independent of shear rate and melt temperature in the shear rate and temperature tested ranges.

ACKNOWLEDGMENTS

The authors would like to thank P. Sammut and A. Derdouri at NRC-IMI for carrying out dynamical mechanical tests and analysis of the LDPE sample.

REFERENCES

1. A.K. Kalkar, H.W. Siesler, F. Pfeifer, and S.A. Wadekar, *Polymer*, **44**, 7251 (2003).
2. M. Zuo, M. Peng, and Q. Zheng, *Polymer*, **46**, 11085 (2005).
3. M. Heinrich, W. Pyckhout-Hintzen, J. Allgaier, D. Richter, E. Straube, T.C.B. McLeish, A. Wiedenmann, R.J. Blackwell, and D.J. Read, *Macromolecules*, **37**, 5054 (2004).
4. M. Baumgaertel and H.H. Winter, *Rheol. Acta*, **28**, 511 (1989).
5. S.H. Jafari, A. Yavari, A. Asadinezhad, H.A. Khonakdar, and F. Bohme, *Polymer*, **46**, 5082 (2005).
6. N. Orbey and J.M. Dealy, *J. Rheol.*, **35**, 1035 (1991).
7. C.L. Rohn, *Analytical Polymer Rheology: Structure-Processing-Property Relationship*, Hanser, Munich, 148 (1995).
8. S.W. Smith, C.K. Hall, and B.D. Freeman, *Phys. Rev. Lett.*, **75**, 1316 (1995).
9. J. Gao and J.H. Weiner, *Macromolecules*, **29**, 6048 (1996).
10. T.H. Yu and G.L. Wilkes, *J. Rheol.*, **40**, 1079 (1996).
11. G. Wiberg, H. Hillborg, and U.W. Gedde, *Polym. Eng. Sci.*, **38**, 1278 (1998).
12. F.L. Colhoun, R.C. Armstrong, and G.C. Rutledge, *Macromolecules*, **35**, 6032 (2002).
13. F.L. Colhoun, R.C. Armstrong, and G.C. Rutledge, *Macromolecules*, **34**, 6670 (2001).
14. G. Wiberg, M.L. Skytt, and U.W. Gedde, *Polymer*, **39**, 2983 (1998).
15. L. Lundberg, B. Stenberg, and J.F. Jansson, *Macromolecules*, **29**, 6256 (1996).
16. R. Edwards and C. Thomas, *Polym. Eng. Sci.*, **41**, 1644 (2001).
17. B. He, X. Yuan, H. Yang, H. Tan, L. Qian, Q. Zhang, and Q. Fu, *Polymer*, **47**, 2448 (2006).
18. A.J. Bur, R.E. Lowry, S.C. Roth, C.L. Thomas, and F.W. Wang, *Macromolecules*, **24**, 3715 (1991).
19. A.J. Bur, R.E. Lowry, S.C. Roth, C.L. Thomas, and F.W. Wang, *Macromolecules*, **25**, 3503 (1992).
20. Y.H. Lee, A.J. Bur, S.C. Roth, P.R. Start, and R.H. Harris, *Polym Adv Technol*, **16**, 249 (2005).
21. P.D. Coates, S.E. Barnes, M.G. Sibley, E.C. Brown, H.G.M. Edwards, and I.J. Scowen, *Polymer*, **44**, 5937 (2003).
22. N.H. Abu-Zahra, *Mechatronics*, **14**, 789 (2004).
23. C. Verdier and M. Piau, *J. Acoust. Soc. Am.*, **101**, 1868 (1997).
24. D. Wang and K. Min, *Polym. Eng. Sci.*, **45**, 998 (2005).
25. L. Piché, A. Hamel, R. Gendron, M. Dumoulin, and J. Tatibouët, U.S. Patent, 5,433,112 (1995).
26. A.J. Bur, S.C. Roth, M.A. Spalding, D.W. Baugh, K.A. Koppi, and W.C. Buzanowski, *Polym. Eng. Sci.*, **44**, 2148 (2004).
27. A.J. Bur and S.C. Roth, *Polym. Eng. Sci.*, **44**, 898 (2004).
28. M.L. Williams, R.F. Landel, and J.D. Ferry, *J. Am. Chem. Soc.*, **77**, 3701 (1995).
29. C.A. Angell, *Polymer*, **38**, 6261 (1997).
30. G. Strobl, *The Physics of Polymers*, *2nd ed.*, Springer, Berlin, Chapter 5.3 (2001).
31. J. Wang, R. Liang, and S. Guo, *Acta Polym. Sin.*, **4**, 422 (1999).

 DOI 10.1002/pen